

Investigating the Capabilities of Popular Turbulence Models in Recreating the Flow Over a Sharp Edged Flat Plate at Incidence

Alasdair Christison Gray*
University of Edinburgh

The complex case of a high angle of attack, slender delta wing in deep water waves has been modelled using Star CCM+ computational fluid dynamics software. In the specified design case the wing was found to exhibit an average lift drag and moment coefficients of 1.1 ± 0.07 , 0.6094 ± 0.0058 and 0.359 ± 0.0064 respectively although the value of the lift coefficient did not appear to converge asymptotically suggesting that more work may be required although the given value does agree well with theoretical predictions in the absence of any usable experimental data. The variation in the lift, drag and moment were all 7-8% somewhat confirming the hypothesis of the delta wing's ability to maintain a constant lift force with the wave induced angle of attack variations. In reality though, a hydrofoil using a traditional wing could achieve the same amount of lift with an order of magnitude less drag and the variation in lift could be minimised with a relatively simple control system. †

I. Introduction

This study aims to model the unsteady flow over a slender delta wing prototype for a marine vehicle and its interaction with a simple wave field. The main focus is on estimating the lift and drag forces acting on the wing and how much variation in these forces occurs due to the wave field. A delta wing has been proposed for the lifting surface of this marine vehicle due to the relatively low variation in lift coefficient with changes in angle of attack of delta wings compared to more traditional wings.

A. Characteristics of Flow Over Slender Delta Wings

The primary features of interest in the flow over a delta wing are the vortices formed at the leading edges of the wing. These leading edge vortices (LEV's) are formed by the curvature and "roll-up" of the two shear layers created as the flow separates round the leading edges (see figure 1a). The low pressures at the cores of these vortices create suction on the delta wing's upper surface, also known as "vortex lift", this is the primary lift generation mechanism for delta wings [1]. The primary difference between the LEV of a delta wing and the 2D LEV seen on a sharp leading edge airfoil (as described by Crompton [2]) is that the delta wing vortices' axes are somewhat aligned with the streamwise direction due to the sweep angle of the leading edge. At low angles of attack the shear layers reattach on the wing surface, similar to the 2D vortex, however as the angle of attack increases, rather than the reattachment point moving past the trailing edge and creating a large wake region, the shear layers collide above the wing centreline (see figure 1b), this means that delta wings can produce relatively stable lift at much higher angles of attack than more traditional wings. The angle of attack at which the shear layers begin to collide is determined by the sweep angle of the wing.

Smaller scale vortices are also formed due to a Kelvin-Helmholtz instability in the shear layer. These alternating vortices are shed close to the leading edge and follow the path of the primary LEV where they are dissipated [3].

B. Design Case

II. Computational Model

The design case being simulated in this study is a delta wing designed to be used as a hydrofoil by a small marine vehicle, the vehicle is moving through a body of deep water in the opposite direction to an oncoming wave field. The wing has an angle of attack of 30° , a sweep angle of 64.5° . The Reynolds and Froude numbers for the design case are given as 50,000 and 0.5048 respectively which, assuming a kinematic viscosity of $\nu = 10^{-6}$, gives a chord length of 0.1 m and a flow speed of 0.5 m s^{-1} . The waves are defined as having a wavelength of 10 chords ($\lambda = 1 \text{ m}$) and a steepness of 0.01, giving a peak to peak amplitude of 1 cm. The apex of the delta wing is 0.2 m (0.2λ) beneath the free surface.

*MEng Student, Department of Mechanical Engineering, A.Gray-17@sms.ed.ac.uk

†All simulation files available at github.com/A-Gray-94/CFD5

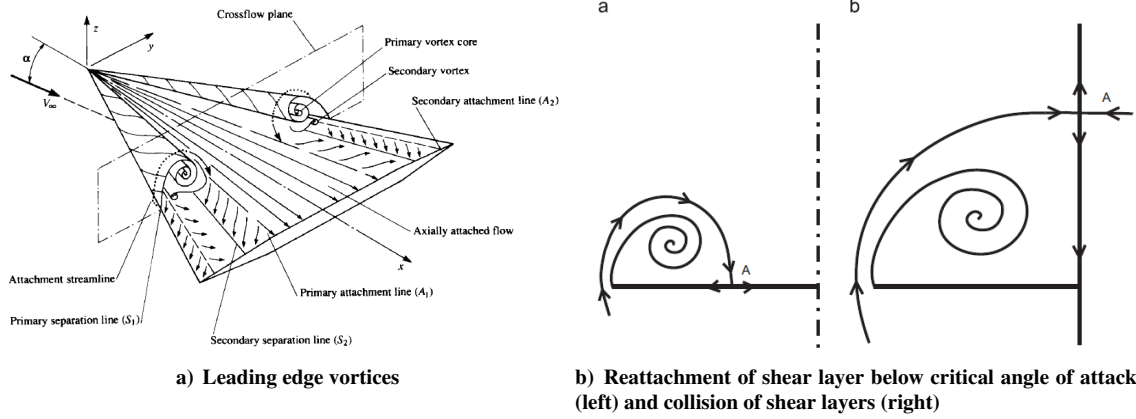


Figure 1. Delta wing flow features

A. Geometry

The wing used in the study was based on the medium radius leading edge wing used by Chu and Luckring of NASA in their extensive experimental program [4]. As such, the radius at the leading and trailing edges are 0.15% of the chord length. This geometry was chosen not only because it was the best defined geometry found in the literature but also because it is known that using a more rounded leading edge reduces the occurrence of unsteady asymmetries in the delta wing LEV's, thus allowing a symmetrical model to be used and significantly reducing the computational cost [5].

A rectangular fluid domain was created, with the upstream and downstream boundaries placed 4 and 15 chordlengths from the wing respectively, the top surface of the domain was placed at the free surface (2 chordlengths above the wing apex) and the lower boundary placed 7 chordlengths below the wing (see figure 2). The domain was made 5 chordlengths wide. These dimensions were based purely on intuition and previous experience modelling airfoil flows but proved to be sufficiently large to avoid any interference of the boundary conditions on the flow around the wing so no other size were tried. It is possible that the size of the domain could have been reduced without any adverse effects but this would not save much computational effort as the vast majority of the grid cells are in the close vicinity of the wing.

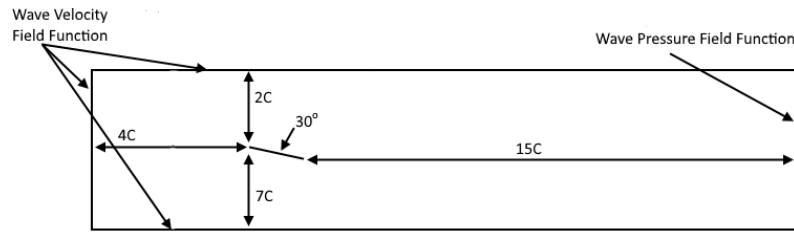


Figure 2. Computational domain and boundary conditions

B. Boundary Conditions

Given that this study involves a wing under the free surface of a body of water with waves, a Volume of Fluid (VOF) model would seem the best choice. However, the VOF model has a great computational cost and it was believed that the relatively large distance between the wing and the free surface and low flow speed meant that the wing would not greatly disturb the free surface. It was therefore decided to implement the flow and wave field using field functions defined by a simple dispersion wave relation:

$$\vec{U} = \begin{bmatrix} u \\ v \\ w \end{bmatrix} = \begin{bmatrix} 0.5 + \frac{H\omega}{2} \sin(qx - \omega t)e^{qy} \\ -\frac{H\omega}{2} \cos(qx - \omega t)e^{qy} \\ 0 \end{bmatrix} \quad (1)$$

$$P = \frac{\rho H \omega^2}{2q} \sin(qx - \omega t) e^{qy} \quad (2)$$

Where $q = 2\pi\lambda$ is the wavenumber, $\omega = \frac{2\pi}{T}$ is the angular wave frequency and H is the peak to peak wave amplitude, the wave period T is found using $\frac{\lambda}{T} = \sqrt{\frac{g\lambda}{2\pi}}$.

To determine which combination of pressure and velocity boundary conditions to apply on the sides of the domain a number of simulations were run on a simple 2D rectangular domain with inviscid flow and the same wave parameters as the design case. It was found that the only discrepancies between the simulation and the analytical flow field occurred near any pressure boundaries and so it was decided that the only pressure boundary should be placed at the domain outlet, furthest away from the wing, whilst the inlet, top and bottom were set as velocity inlets with the velocity defined by equation 1 (see figure 2). Both the remaining sides of the domain were set as symmetry planes.

C. Mesh

A polyhedral mesh was chosen for two primary reasons. Firstly, because of the relatively extreme angle of attack, the flow around the wing would be greatly misaligned with a trimmer mesh, leading to inaccurate results. Additionally, their sudo-random edge orientation and increased number of neighbouring cells compared to tetra or hexahedral cells, improves the computation of gradients and the number of flow directions which polyhedral cells can accurately model making them ideal for recirculating flows, such as the delta wing's LEV [6].

The following mesh sizes were chosen for the "fine" mesh. The target surface size on the wing was set as 2% of the chord but a surface curvature value of 36 points per circle meant that the size at the leading and trailing edges were significantly smaller to accurately capture their curvature. The prism layer was designed to have a sufficient Y^+ value and to have an acceptable volume ratio at its boundary with the freestream cells. The first layer height was chosen as 0.038 mm based on the estimation of an online Y^+ calculator and was found to give Y^+ values below and around 1 over the entire wing. The prism layer growth rate and the number of layers was chosen based on a desired final prism layer cell height, assuming a geometric progression, the height of the n^{th} layer is $a_n = a_1 r^n$ where a_1 is the first layer height and r is the growth rate. Given the desired first and final layer heights and the growth ratio, the required number of prism layers is then:

$$n = \log_r \left(\frac{a_n}{a_1} \right)$$

Using these equations and a desired final layer thickness of 65% of the earlier mention surface size a 25 layer prism mesh with a growth rate of 1.15 was chosen. The surface size on the exterior of the domain were allowed to grow up to 4 times the chordlength a surface and volume expansion rate of 1.2 were set throughout the domain.

A total of 3 grids were created for the study, firstly, all the sizes mentioned above were scaled by 4 and the number of prism layers and the surface curvature value were reduced by a factor of 4 to create a "coarse" grid. This grid was then put through 2 levels of refinement to create the "medium" and "fine" grids. Star CCM+'s polyhedral refinement splits each polyhedral cell into 6 or 7 smaller polyhedra before smoothing the resulting mesh and so the increase in cell numbers is very close to a perfect hexahedral refinement. The coarse, medium and fine grids had 6, 13 and 25 prism layers and 70k, 499k and 3.8m cells respectively.

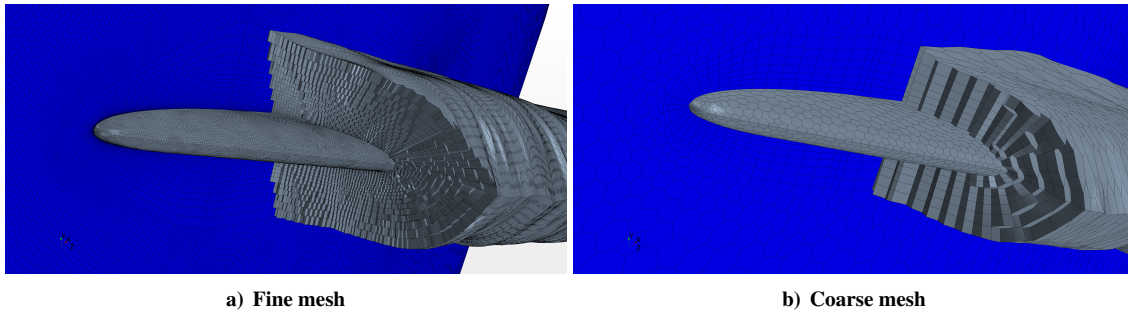


Figure 3. Cut view of the prism layer mesh

D. Physics Models and solvers

The water was modelled as an incompressible liquid and consequently a segregated solver was used. Although the Reynolds number for the design is technically below the critical Reynolds number for airfoils the flow was modelled

as turbulent to represent a more realistic wave field. The turbulent intensity and length scale were specified as 15% and 5 mm (half the peak to peak wave amplitude) at the free surface and were assumed to decrease exponentially with depth at the same rate as the velocity and pressure field functions. The $K-\omega$ SST turbulence model was chosen as both the Spallart-Allmaras and $K-\epsilon$ models are known to be unable to accurately capture the large regions of separated flow that appear in LEV's.

A 2nd order implicit unsteady solver was chosen as the best balance between accuracy and computational cost. An explicit solver would require a CFL number below 1 which, based on the minimum cell size in the fine mesh would require a timestep on the order of 0.1 ms. This would give 8000 time steps per wave period and is therefore infeasible, given that simulations had to run for multiple wave periods. There are therefore two timescales which could guide the choice of timestep for the implicit solver, the wave period and the vortex shedding frequency of the LEV, based on the Strouhal numbers presented by Cummings at the same Reynolds number, the vortex shedding period is likely to be at most 0.02 s and so accurately capturing these vortices would require hundreds of timesteps per wave period. The timestep was therefore chosen as 0.04 s, giving 20 timesteps per wave period. Two further simulations were run with timesteps of 0.02 and 0.08 s. It should therefore be noted that the only unsteady effects expected to be captured in these simulations are those due to the oscillating wave field, higher frequency unsteady effects such as vortex shedding will be smoothed out by the large timestep and the time averaging of the turbulence model.

E. Initial conditions and Running Simulations

All simulations were run as a steady state model for 100 iterations to provide the initial conditions for the unsteady simulations. These were then initially run for 5 seconds and then longer if a steady oscillation in lift and drag forces had not been reached. Each timestep ran for 50 inner iterations or until the continuity residual reached 10^{-4} . All the final simulations were meshed, initialised, run and had data exported using a single batch file, around 8000 csv files were produced which were then processed using Matlab.

III. Results

Uncertainty analysis was performed on the average, minimum and maximum values of the lift, drag and moment coefficients over the last wave period in each simulation. The variation in these quantities due to the timestep changes were at least two orders smaller than the variations due to grid size and were therefore a negligible contribution to the total uncertainty values.

Table 1. Force and moment coefficients

Grid	C_L			C_D			C_M		
	Average	Min	Max	Average	Min	Max	Average	Min	Max
Coarse	1.03	0.991	1.076	0.588	0.564	0.612	0.331	0.319	0.343
Medium	1.06	1.017	1.107	0.601	0.576	0.626	0.347	0.333	0.361
Fine	1.085	1.041	1.13	0.605	0.583	0.627	0.354	0.342	0.366
Extrapolation	1.171	1.047	1.138	0.6094	0.5863	0.6325	0.3589	0.3457	0.3719
Uncertainty	± 0.07	± 0.0102	± 0.012	± 0.0058	± 0.0046	± 0.0074	± 0.0064	± 0.0054	± 0.0075

All of the quantities listed in table 1 showed an order of convergence greater than 1 except for the average lift coefficient (see figure 4b). Consequently the predicted zero grid spacing value of the average lift coefficient is greater than the predicted maximum lift coefficient and should thus be ignored, a more sensible estimate for the average lift coefficient would be ≈ 1.11 . A lift coefficient could not be found for a delta wing with the same sweep angle at the angle of attack and Reynolds number from this design case but using the leading edge suction analogy presented by Polhamus [7] gives a value of 1.126 which agrees very well with the presented results, sitting well within the confidence window. The results predict that the lift, drag and moment coefficients will vary over a typical wave period by 7-8%, whilst this is not disastrous it is not negligible. Figure ?? shows the pressure distributions, time averaged and at the times of maximum and minimum lift, through two spanwise section across the wing, one at 20% of the chord and the other at 60%. In the earlier section there is a very clear suction peak indicating the centre of the leading edge vortex and the pressure values at this point can be seen to vary the most between the maximum and minimum lift times. However moving down to the 60% chord section, not only has the suction peak become smaller but the variation in the pressure distribution between maximum and minimum lift is almost gone. This indicates that as

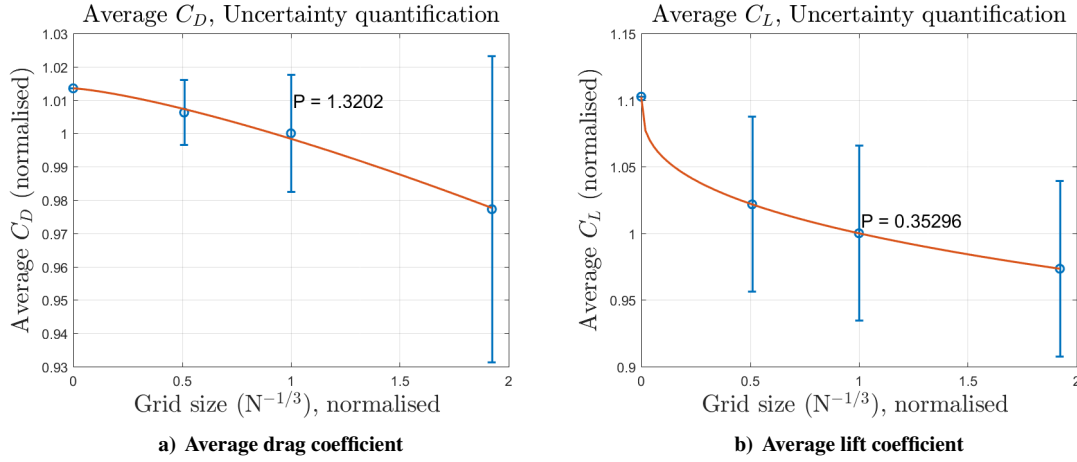


Figure 4. Grid Convergence with uncertainty bars and order of convergence

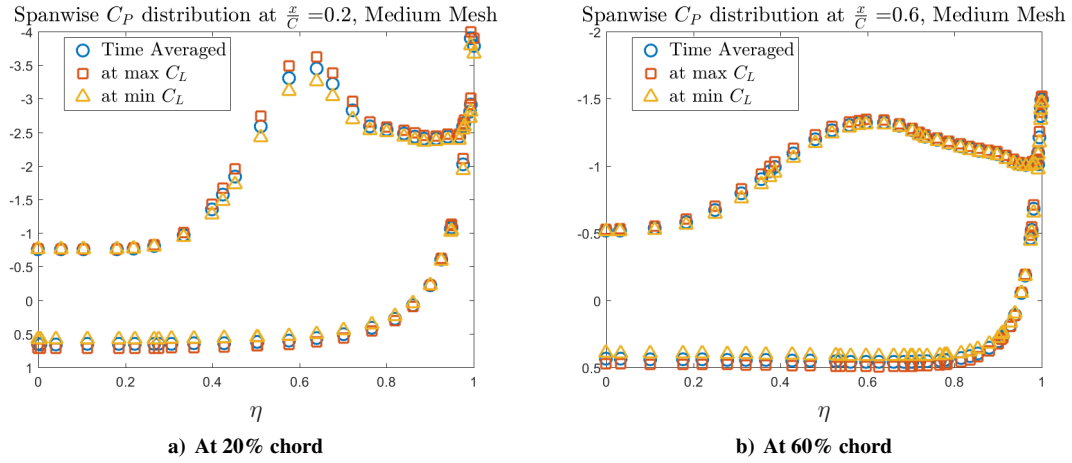


Figure 5. Spanwise pressure coefficient distributions

the LEV moves down the chord it begins to disperse, losing some of its suction, but also that it becomes less sensitive to the angle of attack.

Despite its low lift and drag variation the delta exhibits a poor lift to drag ratio of around 1.8 compared to traditional airfoil which can achieve values of around 10-20 even at low Reynolds numbers as studied in this case. This is why hydrofoil boats typically use traditional airfoils.

IV. Conclusions

The complex case of a high angle of attack, slender delta wing in deep water waves has been modelled using Star CCM+ computational fluid dynamics software. In the specified design case the wing was found to exhibit an average lift drag and moment coefficients of 1.1 ± 0.07 , 0.6094 ± 0.0058 and 0.359 ± 0.0064 respectively although the value of the lift coefficient did not appear to converge asymptotically suggesting that more work may be required although the given value does agree well with theoretical predictions in the absence of any usable experimental data. The variation in the lift, drag and moment were all 7-8% somewhat confirming the hypothesis of the delta wing's ability to maintain a constant lift force with the wave induced angle of attack variations. In reality though, a hydrofoil using a traditional wing could achieve the same amount of lift with an order of magnitude less drag and the variation in lift could be minimised with a relatively simple control system.

With increased computational resources a number of improvements could be made to this study. Firstly, using a significantly smaller timestep and possibly an explicit scheme would allow for the capture of more unsteady effects

like vortex shedding which may create oscillations in the wing forces. Using LES or DES along with a more accurate model of the velocity and turbulence distributions in the wave field would give a more realistic picture of the wing forces rather than a simple sinusoidal variation. It would also be recommended that a VOF simulation be performed where the hull of the boat and the wing mount are present as the interaction between the wing, the hull and the free are likely to greatly affect the forces generated. However for the simple purpose of getting an estimation of the average wing forces the presented simulations are sufficient.

References

- [1] Gursul, I. Ą., Wang, Z., and Vardaki, E., “Review of flow control mechanisms of leading-edge vortices,” *Prog. Aerosp. Sci.*, Vol. 43, 2007, pp. 246–270.
- [2] Crompton, M. J. and Barrett, R. V., “Investigation of the separation bubble formed behind the sharp leading edge of a flat plate at incidence,” *Proc. Inst. Mech. Eng. Part G J. Aerosp. Eng.*, Vol. 214, 2000, pp. 157–176.
- [3] Gordnier, R. E., Visbal, M. R., Force, U. S. A., Air, W.-p., and Base, F., “Unsteady Vortex Structure over a Delta Wing,” Vol. 31, No. 1, 1994.
- [4] Chu, J. and Luckring, J. M., “Experimental Surface Pressure Data Obtained on 65 deg Delta Wing Across Reynolds Number and Mach Number Ranges,” Tech. Rep. February, 1996.
- [5] Cummings, R. M., Forsythe, J. R., Morton, S. A., and Squires, K. D., “Computational challenges in high angle of attack flow prediction,” *Prog. Aerosp. Sci.*, Vol. 39, No. 5, 2003, pp. 369–384.
- [6] Peric, M. and Ferguson, S., “The advantage of polyhedral meshes,” *CD-Adapco*, 2005.
- [7] Polhamus, E., “A concept of the vortex lift of sharp-edge delta wings based on a leading-edge suction analogy,” Tech. rep., NASA, 1966.